

Hidden T -Linear Scattering Rate in $\text{Ba}_{0.6}\text{K}_{0.4}\text{Fe}_2\text{As}_2$ Revealed by Optical Spectroscopy

Y. M. Dai,^{1,2,3} B. Xu,^{1,2} B. Shen,¹ H. Xiao,¹ H. H. Wen,^{1,4} X. G. Qiu,¹ C. C. Homes,^{3,*} and R. P. S. M. Lobo^{2,†}

¹*Beijing National Laboratory for Condensed Matter Physics, Institute of Physics, Chinese Academy of Sciences, P.O. Box 603, Beijing 100190, China*

²*LPEM, ESPCI-ParisTech, CNRS, UPMC, 10 rue Vauquelin, F-75231 Paris Cedex 5, France*

³*Condensed Matter Physics and Materials Science Department, Brookhaven National Laboratory, Upton, New York 11973, USA*

⁴*National Laboratory of Solid State Microstructures and Department of Physics, Nanjing University, Nanjing 210093, China*

(Dated: June 19, 2021)

The optical properties of $\text{Ba}_{0.6}\text{K}_{0.4}\text{Fe}_2\text{As}_2$ have been determined in the normal state for a number of temperatures over a wide frequency range. Two Drude terms, representing two groups of carriers with different scattering rates ($1/\tau$), well describe the real part of the optical conductivity, $\sigma_1(\omega)$. A “broad” Drude component results in an incoherent background with a T -independent $1/\tau_b$, while a “narrow” Drude component reveals a T -linear $1/\tau_n$ resulting in a resistivity $\rho_n \equiv 1/\sigma_{1n}(\omega \rightarrow 0)$ also linear in temperature. An $\arctan(T)$ low-frequency spectral weight is also a strong evidence for a T -linear $1/\tau$. Comparison to other materials with similar behavior suggests that the T -linear $1/\tau_n$ and ρ_n in $\text{Ba}_{0.6}\text{K}_{0.4}\text{Fe}_2\text{As}_2$ originate from scattering from spin fluctuations and hence that an antiferromagnetic quantum critical point is likely to exist in the superconducting dome.

PACS numbers: 72.15.-v, 74.70.-b, 78.30.-j

Over the last several decades, it has been observed that the electrical resistivity ρ of some strongly-correlated materials increases linearly with temperature (T -linear ρ), particularly in the vicinity of an antiferromagnetic quantum critical point (QCP), a striking deviation from Landau’s Fermi-liquid description of metals. This anomalous T -linear ρ , extensively studied in the high- T_c cuprate superconductors [1–4], organic Bechgaard salts [5, 6], as well as heavy-fermion metals [7–10], may be intimately related to the emergence of superconductivity [4, 5, 11]. It is generally believed that in proximity to the antiferromagnetic QCP, spin fluctuations are so strong that the scattering process of quasiparticles is severely modified, inducing non-Fermi-liquid behavior. Such spin fluctuations may be responsible for the pairing of electrons in high- T_c superconductors [12–14].

The presence of the T -linear ρ and a QCP in the newly discovered iron-based superconductors is highly desired since superconductivity arises in the vicinity of the spin-density-wave (SDW) instability [15, 16]. Up to this point, T -linear ρ has been observed by transport, arousing considerable effort to describe it as evidence of possible quantum criticality in iron-pnictides, especially in the “122” family [5, 17–23]. However, unlike the high- T_c cuprates, iron-pnictides fall into the category of multi-band materials [24, 25]. Up to five Fe-3d bands crossing the Fermi level contribute to the Fermi surface, leading to the presence of three hole-like Fermi pockets at Γ -point and two electron-like pockets at the corners of Brillouin zone. The scattering rate $1/\tau$ and the response of quasiparticles to external electrical field may vary considerably in different Fermi pockets [19, 26–28]. As a result, the transport properties become extremely complicated in such

a system and the question of whether a T -linear ρ in iron-pnictides originates from multi-band effects or the presence of a QCP makes it inadequate to investigate the transport properties alone in search of a non-Fermi-liquid behavior and evidence for possible QCP [28, 29].

Although many optical studies on iron-pnictides have been reported [30–32], the above issue has never been touched due to the absence of detailed T dependent optical data. In this Letter we address this issue by studying the detailed T dependence of the optical conductivity and low-frequency spectral weight in $\text{Ba}_{0.6}\text{K}_{0.4}\text{Fe}_2\text{As}_2$. The low-frequency optical conductivity is described by two Drude terms: a broad Drude with a large $1/\tau_b$ that is basically T -independent alongside a narrow one with a small T -linear $1/\tau_n$ that reveals a $\rho_n \equiv 1/\sigma_{1n}(\omega \rightarrow 0) \propto T$. The low-frequency spectral weight increases with cooling, following an $\arctan(T)$ dependence, which is demonstrated to be a clear signature of T -linear $1/\tau$. Comparison with similar behavior found in other materials attributes the T -linear $1/\tau_n$ and ρ_n in $\text{Ba}_{0.6}\text{K}_{0.4}\text{Fe}_2\text{As}_2$ to spin fluctuation scattering and the presence of a QCP in the superconducting dome.

High quality $\text{Ba}_{0.6}\text{K}_{0.4}\text{Fe}_2\text{As}_2$ single crystals were grown using a self-flux method [19]. The inset of Fig. 1 shows the DC resistivity of $\text{Ba}_{0.6}\text{K}_{0.4}\text{Fe}_2\text{As}_2$ as a function of temperature. The $\rho(T)$ curve is characterized by a sharp superconducting transition at $T_c \simeq 39$ K and a tendency to saturation at room temperature. A visible change in slope occurs at about 175 K.

The near-normal incident reflectance, $R(\omega)$, has been measured for light polarized in the a - b plane using FTIR spectrometers and an *in situ* evaporation technique [33]. Data from $\simeq 20 - 12000 \text{ cm}^{-1}$ were col-

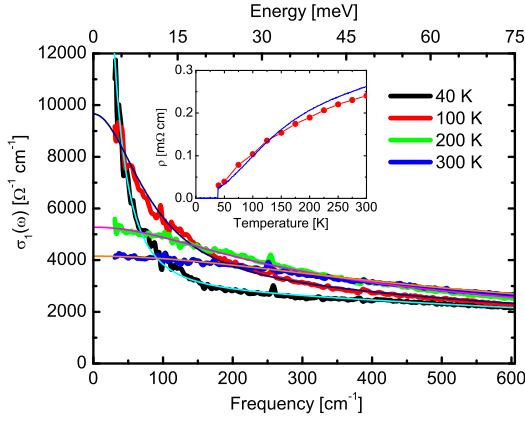


Figure 1. (color online) The thick solid lines in the main panel are ab -plane $\sigma_1(\omega)$ of $\text{Ba}_{0.6}\text{K}_{0.4}\text{Fe}_2\text{As}_2$ at different temperatures in the normal state. The smooth lines through the data are fits with Drude-Lorentz model. The inset shows the DC resistivity as a function of temperature from transport measurement (solid curve) and the values derived from the zero frequency extrapolation of $\sigma_1(\omega)$ (solid circles).

lected at 18 different temperatures from 5 to 300 K on a freshly cleaved surface. The visible and UV range ($10\,000 - 55\,000\text{ cm}^{-1}$) $R(\omega)$ was measured at room temperature with an AvaSpec-2048 \times 14 fiber optic spectrometer. The real part of the complex optical conductivity, $\sigma_1(\omega)$, is determined from $R(\omega)$ via Kramers-Kronig analysis. A Hagen-Rubens form ($R = 1 - A\sqrt{\omega}$) is used for the low-frequency extrapolation. At high frequencies, $R(\omega)$ is assumed to be constant to 40 eV, above which a free-electron response (ω^{-4}) is used.

The main panel of Fig. 1 shows $\sigma_1(\omega)$ at 4 selected temperatures in the normal state (thick solid lines); all the spectra exhibit the well-known Drude-like metallic response. In order to quantitatively analyze the optical data, we fit $\sigma_1(\omega)$ to the Drude-Lorentz model,

$$\sigma_1(\omega) = \frac{2\pi}{Z_0} \left[\sum_k \frac{\Omega_{p,k}^2}{\tau_k(\omega^2 + \tau_k^{-2})} + \sum_j \frac{\gamma_j \omega^2 \Omega_j^2}{(\omega_j^2 - \omega^2)^2 + \gamma_j^2 \omega^2} \right] \quad (1)$$

where Z_0 is the vacuum impedance. The first term describes a sum of free-carrier Drude responses, each characterized by a plasma frequency $\Omega_p^2 = 4\pi n e^2 / m^*$, where n is a carrier concentration and m^* is an effective mass, and a scattering rate $1/\tau$. The second term corresponds to a sum of Lorentz oscillators characterized by a resonance frequency (ω_j), a line width (γ_j) and an oscillator strength (Ω_j). This Drude-Lorentz model is also used to determine the dc properties of the system [34].

As shown in Fig. 2, $\sigma_1(\omega)$ at 150 K is described by a broad Drude with a large scattering rate $1/\tau_b \approx 936\text{ cm}^{-1}$, and a narrow Drude with a small scattering rate $1/\tau_n \approx 158\text{ cm}^{-1}$ and an overdamped Lorentzian term. The linear superposition of these three components

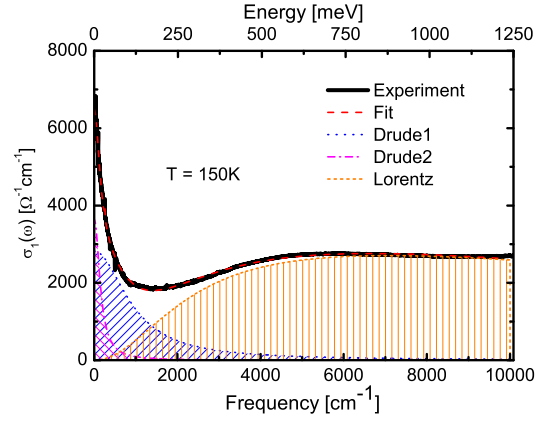


Figure 2. (color online) The black solid curve is the measured $\sigma_1(\omega)$ of $\text{Ba}_{0.6}\text{K}_{0.4}\text{Fe}_2\text{As}_2$ at 150 K. The red dashed line through the data is the fit which is decomposed into a broad Drude (blue dotted line), a narrow Drude (pink dotted-dashed line) and a Lorentz (orange short-dashed line) term.

gives very good description to $\sigma_1(\omega)$ up to $10\,000\text{ cm}^{-1}$ at all the measured temperatures in the normal state. Fits for other temperatures are selectively shown in the main panel of Fig. 1 as smooth thin lines through the corresponding data. The inset of Fig. 1 compares the optical estimate for the DC resistivity $\rho \equiv 1/\sigma_1(\omega \rightarrow 0)$ (solid circles) to the transport measurements (solid line).

The two-Drude fit indicates the existence of two groups of carriers with different $1/\tau$'s in $\text{Ba}_{0.6}\text{K}_{0.4}\text{Fe}_2\text{As}_2$, which was first pointed out by Wu *et al.* in various iron-pnictides [35]. The disparity of the $1/\tau$'s in different bands is also supported by both theoretical calculations [36] and measurements using other techniques on similar materials [19, 26–28]. Tu *et al.* suggest that it is appropriate to describe the broad Drude term as bound excitations [37], because the mean free path $l = v_F \tau$ (v_F is the Fermi velocity) associated with the broad Drude is less than the shortest interatomic spacing, violating the Mott-Ioffe-Regel condition [38]. In $\text{Ba}_{0.6}\text{K}_{0.4}\text{Fe}_2\text{As}_2$, the average Fermi velocities of the electron and hole pockets are estimated to be $v_F^e \simeq 0.40\text{ eV\AA}$ and $v_F^h \simeq 0.36\text{ eV\AA}$ [39], respectively. Furthermore, it is reported that in iron-pnictides holes have a larger $1/\tau$ than electrons [19, 26–28]. If we associate the broad Drude component ($1/\tau_b \simeq 936\text{ cm}^{-1}$) with the hole pockets, a mean free path of $l_h \simeq 3\text{ \AA}$ is obtained. This value is close to the lattice parameter $a \simeq 4\text{ \AA}$ of the 122 family compounds and probably too small for coherent transport. Since the broad Drude only produces an incoherent, T -independent, background contribution to the total $\sigma_1(\omega)$, the nature of the broad Drude component (whether or not bound excitations) does not affect our analysis on the temperature dependence of $\sigma_1(\omega)$ and low-frequency spectral weight.

The temperature dependence of the two Drude components provides information about the nature of the

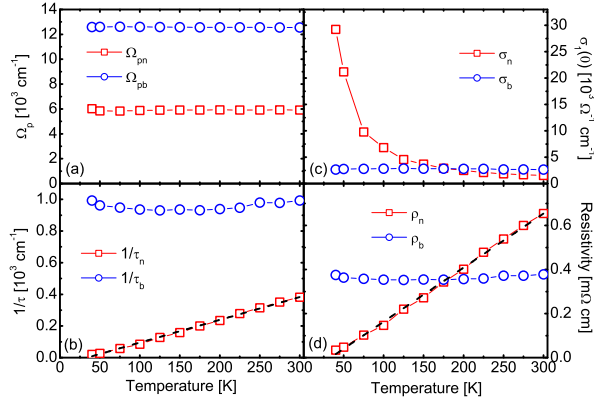


Figure 3. (color online) The T dependence of (a) the plasma frequency Ω_p , (b) the scattering rate $1/\tau$, (c) the contribution to DC conductivity $\sigma_1(\omega \rightarrow 0)$, and (d) the equivalent resistivity ρ for the narrow and broad Drude components, respectively. The dashed lines in panels (b) and (d) are linear fits to $1/\tau_n$ and ρ_n , respectively.

two different types of carriers in this material. Figure 3 shows the T dependence of the Drude parameters from our fits. The subscripts n and b stand for the narrow and broad Drude terms, respectively. Fig. 3(a) shows the T dependence of the plasma frequencies of the two Drude terms. Upon cooling, Ω_p is roughly a constant for each of the two components, indicating that the band structure and n/m^* does not change with temperature, in agreement with a previous work [35]. Fig. 3(b) portrays the T dependence of the scattering rate of the two Drude components, where $1/\tau_b$ is basically T -independent while $1/\tau_n \propto T$; the black dashed line denotes a linear fit. Fig. 3(c) displays the contribution of the two groups of carriers to the DC conductivity. As the broad Drude (σ_b) is T -independent, the temperature dependence of the total DC conductivity arises out of the narrow Drude band (σ_n). The $\rho(T)$ curve of $\text{Ba}_{0.6}\text{K}_{0.4}\text{Fe}_2\text{As}_2$, shown in the inset of Fig. 1, exhibits a tendency to saturation at room temperature, and a change of slope can be seen at about 175 K. This behavior can be explained by the different T dependence of the two Drude bands, which can be considered as a parallel-circuit [40]: $\sigma = \sigma_n + \sigma_b$. A crossover-region, where $\sigma_n \simeq \sigma_b$, is found in Fig. 3(c) at $\simeq 175$ K. Below this temperature, $\sigma_n > \sigma_b$, so the total DC conductivity is dominated by σ_n which exhibits strong temperature dependence. As a result, below 175 K, $\rho(T)$ decreases quickly with decreasing temperature. Above 175 K, $\sigma_n < \sigma_b$, and the total DC conductivity is dominated by σ_b which shows no temperature dependence. Hence, above 175 K, the growth of the DC resistivity slows with heating, resulting in the change of slope and the tendency to saturation in $\rho(T)$. Similar conclusions were obtained from investigations of the Hall effect [28, 29] and theoretical calculations [41]. In the $\omega \rightarrow 0$ limit, the inverse of $\sigma_1(0)$ yields the re-

sistivity from the two Drude components, as shown in Fig. 3(d). The resistivity of the broad Drude remains a constant at all measured temperatures, while a T -linear ρ_n is revealed for the narrow Drude component. This is in accord with transport measurements on hole-doped 122 compounds [18–20], where T -linear ρ was observed at low temperatures in optimally-doped materials. The T -linear ρ is only found at low temperatures as this is the region dominated by the narrow Drude component.

Further evidence for T -linear $1/\tau$ lies in the temperature dependence of the low-frequency spectral weight. The spectral weight is defined as

$$W_0^{\omega_c} = \int_0^{\omega_c} \sigma_1(\omega) d\omega, \quad (2)$$

where ω_c is a cutoff frequency. In a Drude metal the scattering rate decreases upon cooling, producing a narrowing of the Drude response and an increase of the DC conductivity, resulting in a transfer of spectral weight from high to low frequencies and an increase in $W_0^{\omega_c}$. To quantitatively analyze the T dependence of the low-frequency spectral weight, we adopt one Drude optical conductivity [see Eq. (1)] into Eq. (2), to obtain the spectral weight as a function of $1/\tau$

$$W_0^{\omega_c}(1/\tau) = \frac{2\pi\Omega_p^2}{Z_0} \arctan(\omega_c\tau). \quad (3)$$

In the case of $1/\tau \propto T$, Eq. (3) can be simplified as

$$W_0^{\omega_c}(T) = a_1 \arctan\left(\frac{a_2}{T}\right), \quad (4)$$

where $a_1 = 2\pi\Omega_p^2/Z_0$, and $a_2 \propto \omega_c$; both are T -independent parameters. Considering the spectral weight arising from the incoherent part and inter-band transition (Lorentz), which are both T -independent, we introduce the third T -independent parameter a_0 into Eq. (4). Finally, the low-frequency spectral weight as a function of temperature for $1/\tau \propto T$ is written as

$$W_0^{\omega_c}(T) = a_0 + a_1 \arctan\left(\frac{a_2}{T}\right). \quad (5)$$

$W_0^{\omega_c}$ can be easily determined by integrating the measured $\sigma_1(\omega)$. The open symbols in Fig. 4 denote $W_0^{\omega_c}$ with different ω_c 's: 150 (squares), 200 (triangles) and 250 cm^{-1} (diamonds). As expected in a metallic system, for all the ω_c 's, $W_0^{\omega_c}$ increases with decreasing T . The solid curves through the data are the least square fits using Eq. (5). The excellent agreement indicates that a T -linear $1/\tau$ dominates the low frequency $\sigma_1(\omega)$ over a very broad temperature range.

We now discuss the possible origin of the T -linear $1/\tau_n$ and ρ_n . A T -linear ρ is usually expected in a system dominated by electron-phonon scattering in the regime $T \gg \Theta_D$, where Θ_D is the Debye temperature; in the regime $T < \Theta_D$, the resistivity is approximated by a

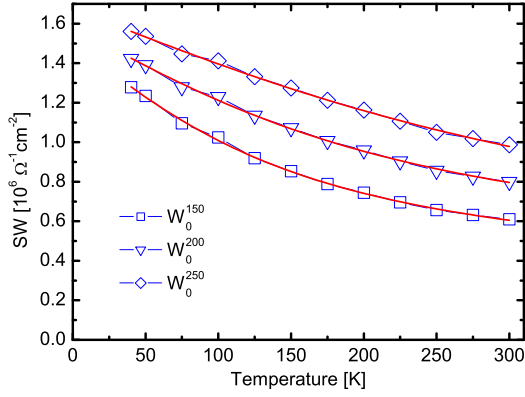


Figure 4. (color online) Temperature dependence of the low-frequency spectral weight $W_0^{\omega_c}$ with different ω_c 's: 150 (squares), 200 (triangles) and 250 cm^{-1} (diamonds). The solid lines through the data represent the expected temperature dependence for $1/\tau \propto T$ at each ω_c .

low-order polynomial that is neither linear nor quadratic in temperature. Transport measurements in the 122 compounds suggest $\Theta_D \simeq 250$ K [37, 42]. However, the T -linear $1/\tau_n$ and ρ_n spans a very broad temperature range, from T_c up to 300 K, which is inconsistent with the electron-phonon dominated scattering process. Further clues on the T -linear $1/\tau_n$ and ρ_n may be revealed by an examination of the phase diagram of the $\text{Ba}_{1-x}\text{K}_x\text{Fe}_2\text{As}_2$ system and a comparison with similar behavior found in other materials. The parent compound BaFe_2As_2 orders in an SDW state below $T_{SDW} \approx 138$ K; T_{SDW} is suppressed by K doping allowing superconductivity to emerge. Here, $1/\tau_n \propto T$ is observed at the doping where the SDW order is entirely suppressed, i.e. $T_{SDW} \rightarrow 0$. At this point, spin fluctuations are expected to be very strong, which has been experimentally confirmed by NMR [43–45]. This brings us to models that attribute T -linear ρ to spin-fluctuation scattering [13, 46]. The T -linear ρ (or $1/\tau$) is also found in cuprates such as Nd-doped $\text{La}_{2-x}\text{Sr}_x\text{CuO}_4$ [3] and electron-doped $\text{La}_{2-x}\text{Ce}_x\text{CuO}_4$ [4], organic superconductors $(\text{TMTSF})_2\text{PF}_6$ [5] and $(\text{TMTSF})_2\text{ClO}_4$ [6], as well as a number of heavy fermions such as CeCoIn_5 [7, 8] and YbRh_2Si_2 [9, 10]. Studies on these materials have shown that T -linear ρ , arising on the border of antiferromagnetic order, is caused by spin-fluctuation scattering due to the proximity of an antiferromagnetic QCP. Studies on cuprates and Bechgaard salts [4, 11] further show that the strength (or coefficient) of the T -linear ρ scales with T_c and disappears upon approaching the point where $T_c \rightarrow 0$, suggestive of intimate relation between the T -linear ρ and superconductivity. Anomalous T -linear ρ (or $1/\tau$) and pairing in unconventional superconductors may share a common origin: spin fluctuations. The hidden T -linear $1/\tau_n$ and ρ_n in $\text{Ba}_{0.6}\text{K}_{0.4}\text{Fe}_2\text{As}_2$ revealed by optical measurements may have the same origin as those found in

the cuprates, organic superconductors and heavy fermion metals, because these materials share strikingly similar phase diagrams. Our observations may also imply a possible QCP in the superconducting dome. The existence of the QCP in iron-pnictides is supported by transport properties [18–20], NMR studies [43, 44], de Haas-van Alphen effect [47], penetration depth measurement [21] and first-principles calculations [17].

Spin-fluctuation induced T -linear ρ suggests an equivalent ω -linear $1/\tau(\omega)$ [13], obtainable through the extended Drude model provided that interband contribution is negligible. Low energy interband transitions are important in iron-pnictides, and their contribution has to be subtracted to determine $1/\tau(\omega)$ for mobile carriers [32, 48]. We calculated $1/\tau(\omega)$ via the extended Drude model with the interband contribution subtracted (supplementary) and found that by taking into account the interband transitions, a large fraction of the frequency dependence in $1/\tau(\omega)$ is eliminated, which is consistent with Charnukha *et al.*'s analysis on $\text{Ba}_{0.68}\text{K}_{0.32}\text{Fe}_2\text{As}_2$ [32]. There is no confident evidence for the expected ω -linear $1/\tau(\omega)$, since it could be masked by the multiband character of the iron-pnictides.

In order to check if the T -linear $1/\tau$ is unique in $\text{Ba}_{0.6}\text{K}_{0.4}\text{Fe}_2\text{As}_2$ or general in iron-pnictides, we applied the same analysis to $\text{BaFe}_2(\text{As}_{0.7}\text{P}_{0.3})_2$ (supplementary). Interestingly, T -linear $1/\tau$ is also found for the narrow Drude. This suggests that T -linear $1/\tau$ is not unique in $\text{Ba}_{0.6}\text{K}_{0.4}\text{Fe}_2\text{As}_2$, but most likely, a general behavior in iron-pnictides at the doping where SDW order is completely suppressed, i.e. $T_{SDW} \rightarrow 0$.

In summary, the detailed T dependence of the normal state $\sigma_1(\omega)$ and low-frequency spectral weight in $\text{Ba}_{0.6}\text{K}_{0.4}\text{Fe}_2\text{As}_2$ have been examined. Two Drude components with different $1/\tau$'s yield an excellent description of the low-frequency optical response, indicating the existence of two groups of carriers with different quasi-particle lifetimes. The broad Drude component produces an incoherent background conductivity with no temperature dependence, while the narrow Drude component reveals a T -linear $1/\tau_n$ and ρ_n . This fact explains the T -linear ρ behavior at low temperatures and the tendency to saturation at room temperature observed in transport measurements in optimally hole-doped 122 compounds. An arctan(T) dependence of the low-frequency spectral weight is also a strong evidence for a T -linear $1/\tau$. Comparison with similar behavior found in other materials suggests that the T -linear $1/\tau_n$ and ρ_n in $\text{Ba}_{0.6}\text{K}_{0.4}\text{Fe}_2\text{As}_2$ may arise out of spin-fluctuation scattering due to the possible existence of an antiferromagnetic QCP in the superconducting dome.

We thank Hu Miao, Xiaoxiang Xi, Wei Ku, Cong Ren and Lei Shan for helpful discussion. Work in Beijing was supported by the NSFC (No. 91121004 and No. 11104335) and the MSTC (973 Projects No. 2011CBA00107, No. 2012CB821400, No. 2012CB921302

and No. 2009CB929102). Work at BNL was supported by the U.S. Department of Energy, Office of Basic Energy Sciences, Division of Materials Sciences and Engineering under Contract No. DE-AC02-98CH10886. We acknowledge the financial support from the Science and Technology Service of the French Embassy in China.

* homes@bnl.gov

† lobo@espci.fr

- [1] G. S. Boebinger, *Science* **323**, 590 (2009).
- [2] R. A. Cooper, Y. Wang, B. Vignolle, O. J. Lipscombe, S. M. Hayden, Y. Tanabe, T. Adachi, Y. Koike, M. Nohara, H. Takagi, C. Proust, and N. E. Hussey, *Science* **323**, 603 (2009).
- [3] R. Daou, N. Doiron-Leyraud, D. LeBoeuf, S. Y. Li, F. Laliberte, O. Cyr-Choiniere, Y. J. Jo, L. Balicas, J.-Q. Yan, J.-S. Zhou, J. B. Goodenough, and L. Taillefer, *Nat. Phys.* **5**, 31 (2009).
- [4] K. Jin, N. P. Butch, K. Kirshenbaum, J. Paglione, and R. L. Greene, *Nature* **476**, 73 (2011).
- [5] N. Doiron-Leyraud, P. Auban-Senzier, S. René de Cotret, C. Bourbonnais, D. Jérôme, K. Bechgaard, and L. Taillefer, *Phys. Rev. B* **80**, 214531 (2009).
- [6] N. Doiron-Leyraud, P. Auban-Senzier, S. R. de Cotret, A. Sedeki, C. Bourbonnais, D. Jérôme, K. Bechgaard, and L. Taillefer, (2009), arXiv:0905.0964 (unpublished).
- [7] A. Malinowski, M. F. Hundley, C. Capan, F. Ronning, R. Movshovich, N. O. Moreno, J. L. Sarrao, and J. D. Thompson, *Phys. Rev. B* **72**, 184506 (2005).
- [8] M. A. Tanatar, J. Paglione, C. Petrovic, and L. Taillefer, *Science* **316**, 1320 (2007).
- [9] O. Trovarelli, C. Geibel, S. Mederle, C. Langhammer, F. M. Grosche, P. Gegenwart, M. Lang, G. Sparn, and F. Steglich, *Phys. Rev. Lett.* **85**, 626 (2000).
- [10] P. Gegenwart, J. Custers, C. Geibel, K. Neumaier, T. Tayama, K. Tenya, O. Trovarelli, and F. Steglich, *Phys. Rev. Lett.* **89**, 056402 (2002).
- [11] L. Taillefer, *Annual Review of Condensed Matter Physics* **1**, 51 (2010).
- [12] P. Monthoux, D. Pines, and G. G. Lonzarich, *Nature* **450**, 1177 (2007).
- [13] T. Moriya and K. Ueda, *Adv. Phys.* **49**, 555 (2000).
- [14] I. I. Mazin, D. J. Singh, M. D. Johannes, and M. H. Du, *Phys. Rev. Lett.* **101**, 057003 (2008).
- [15] Y. Kamihara, T. Watanabe, M. Hirano, and H. Hosono, *J. Am. Chem. Soc.* **130**, 3296 (2008).
- [16] M. Rotter, M. Tegel, and D. Johrendt, *Phys. Rev. Lett.* **101**, 107006 (2008).
- [17] G. Xu, H. Zhang, X. Dai, and Z. Fang, *EPL* **84**, 67015 (2008).
- [18] M. Gooch, B. Lv, B. Lorenz, A. M. Guloy, and C.-W. Chu, *Phys. Rev. B* **79**, 104504 (2009).
- [19] B. Shen, H. Yang, Z.-S. Wang, F. Han, B. Zeng, L. Shan, C. Ren, and H.-H. Wen, *Phys. Rev. B* **84**, 184512 (2011).
- [20] J. Maiwald, H. S. Jeevan, and P. Gegenwart, *Phys. Rev. B* **85**, 024511 (2012).
- [21] K. Hashimoto, K. Cho, T. Shibauchi, S. Kasahara, Y. Mizukami, R. Katsumata, Y. Tsuruhara, T. Terashima, H. Ikeda, M. A. Tanatar, H. Kitano, N. S. Lovich, R. W. Giannetta, P. Walmsley, A. Carrington, R. Prozorov, and Y. Matsuda, *Science* **336**, 1554 (2012).
- [22] S. Kasahara, T. Shibauchi, K. Hashimoto, K. Ikeda, S. Tonegawa, R. Okazaki, H. Shishido, H. Ikeda, H. Takeya, K. Hirata, T. Terashima, and Y. Matsuda, *Phys. Rev. B* **81**, 184519 (2010).
- [23] T. Shibauchi, A. Carrington, and Y. Matsuda, (2013), arXiv:1304.6387 (unpublished).
- [24] D. J. Singh and M.-H. Du, *Phys. Rev. Lett.* **100**, 237003 (2008).
- [25] H. Ding, P. Richard, K. Nakayama, K. Sugawara, T. Arakane, Y. Sekiba, A. Takayama, S. Souma, T. Sato, T. Takahashi, Z. Wang, X. Dai, Z. Fang, G. F. Chen, J. L. Luo, and N. L. Wang, *EPL* **83**, 47001 (2008).
- [26] L. Fang, H. Luo, P. Cheng, Z. Wang, Y. Jia, G. Mu, B. Shen, I. I. Mazin, L. Shan, C. Ren, and H.-H. Wen, *Phys. Rev. B* **80**, 140508 (2009).
- [27] B. Muschler, W. Prestel, R. Hackl, T. P. Devereaux, J. G. Analytis, J.-H. Chu, and I. R. Fisher, *Phys. Rev. B* **80**, 180510 (2009).
- [28] F. Rullier-Albenque, D. Colson, A. Forget, P. Thuéry, and S. Poissonnet, *Phys. Rev. B* **81**, 224503 (2010).
- [29] F. Rullier-Albenque, D. Colson, A. Forget, and H. Aloul, *Phys. Rev. Lett.* **103**, 057001 (2009).
- [30] G. Li, W. Z. Hu, J. Dong, Z. Li, P. Zheng, G. F. Chen, J. L. Luo, and N. L. Wang, *Phys. Rev. Lett.* **101**, 107004 (2008).
- [31] A. Charnukha, P. Popovich, Y. Matiks, D. L. Sun, C. T. Lin, A. N. Yaresko, B. Keimer, and A. V. Boris, *Nat Commun* **2**, 219 (2011).
- [32] A. Charnukha, O. V. Dolgov, A. A. Golubov, Y. Matiks, D. L. Sun, C. T. Lin, B. Keimer, and A. V. Boris, *Phys. Rev. B* **84**, 174511 (2011).
- [33] C. C. Homes, M. Reedyk, D. A. Crandles, and T. Timusk, *Applied Optics* **32**, 2976 (1993).
- [34] D. B. Romero, C. D. Porter, D. B. Tanner, L. Forro, D. Mandrus, L. Mihaly, G. L. Carr, and G. P. Williams, *Phys. Rev. Lett.* **68**, 1590 (1992).
- [35] D. Wu, N. Barišić, P. Kallina, A. Faridian, B. Gorshunov, N. Drichko, L. J. Li, X. Lin, G. H. Cao, Z. A. Xu, N. L. Wang, and M. Dressel, *Phys. Rev. B* **81**, 100512 (2010).
- [36] A. F. Kemper, M. M. Korshunov, T. P. Devereaux, J. N. Fry, H.-P. Cheng, and P. J. Hirschfeld, *Phys. Rev. B* **83**, 184516 (2011).
- [37] J. J. Tu, J. Li, W. Liu, A. Punnoose, Y. Gong, Y. H. Ren, L. J. Li, G. H. Cao, Z. A. Xu, and C. C. Homes, *Phys. Rev. B* **82**, 174509 (2010).
- [38] M. Gurvitch, *Phys. Rev. B* **24**, 7404 (1981).
- [39] H. Ding, K. Nakayama, P. Richard, S. Souma, T. Sato, T. Takahashi, M. Neupane, Y.-M. Xu, Z.-H. Pan, A. V. Fedorov, Z. Wang, X. Dai, Z. Fang, G. F. Chen, J. L. Luo, and N. L. Wang, *Journal of Physics: Condensed Matter* **23**, 135701 (2011).
- [40] H. Wiesmann, M. Gurvitch, H. Lutz, A. Ghosh, B. Schwarz, M. Strongin, P. B. Allen, and J. W. Halley, *Phys. Rev. Lett.* **38**, 782 (1977).
- [41] A. Golubov, O. Dolgov, A. Boris, A. Charnukha, D. Sun, C. Lin, A. Shevchun, A. Korobenko, M. Trunin, and V. Zverev, *JETP Letters* **94**, 333 (2011).
- [42] N. Ni, S. L. Bud'ko, A. Kreyssig, S. Nandi, G. E. Rustan, A. I. Goldman, S. Gupta, J. D. Corbett, A. Kracher, and P. C. Canfield, *Phys. Rev. B* **78**, 014507 (2008).
- [43] F. L. Ning, K. Ahilan, T. Imai, A. S. Sefat, M. A. McGuire, B. C. Sales, D. Mandrus, P. Cheng, B. Shen,

- and H.-H. Wen, Phys. Rev. Lett. **104**, 037001 (2010).
- [44] Y. Nakai, T. Iye, S. Kitagawa, K. Ishida, H. Ikeda, S. Kasahara, H. Shishido, T. Shibauchi, Y. Matsuda, and T. Terashima, Phys. Rev. Lett. **105**, 107003 (2010).
 - [45] Z. Li, D. L. Sun, C. T. Lin, Y. H. Su, J. P. Hu, and G.-q. Zheng, Phys. Rev. B **83**, 140506 (2011).
 - [46] S. Sachdev and B. Keimer, Phys. Today **64**, 29 (2011).
 - [47] P. Walmsley, C. Putzke, L. Malone, I. Guilmón, D. Vignolles, C. Proust, S. Badoux, A. I. Coldea, M. D. Watson, S. Kasahara, Y. Mizukami, T. Shibauchi, Y. Matsuda, and A. Carrington, Phys. Rev. Lett. **110**, 257002 (2013).
 - [48] L. Benfatto, E. Cappelluti, L. Ortenzi, and L. Boeri, Phys. Rev. B **83**, 224514 (2011).